Available online at www.sciencedirect.com
ScienceDirect
Journal of Nuclear Materials 362 (2007) 60–74
journal of nuclear materials
www.elsevier.com/locate/jnucmat

Disproportionation of Pu(IV): A reassessment of kinetic and equilibrium properties

John M. Haschke *

Actinide Science Consulting, P.O. Box 96, Harwood, TX 78632, USA

Received 11 July 2006; accepted 14 November 2006

Abstract

Kinetic results for disproportionation of Pu(VI) and reaction of Pu(III) with Pu(VI) show that rates of $3Pu^{4+}$ (aq) + $2H_2O$ (l) = $2Pu^{3+}$ (aq) + PuO_2^{2+} (aq) + $4H^+$ (aq) in HNO_3 and $HClO_4$ solutions are described by trimolecular rate laws consistent with involvement of trimeric hydroxo complexes as reactive intermediates in the slow mechanistic steps. Product ratios and modeling of concentration–time curves reveal that Pu(V) is formed by reduction of Pu(VI) product in a secondary reaction. Results do not support the accepted interpretation that attributes reversible reaction and Pu(V) formation to a two-step bimolecular process. Secondary redox reactions driven by disproportionation of Pu(VI) prevent attainment of equilibrium in 1 M H^+ and determine long-term redox chemistry. The equilibrium constant (0.00051) defined by forward and reverse rate constants for 1 M $HClO_4$ agrees with that (0.00049) derived from concentration data for 1 M HNO_3, but not with prior results. Disagreement of these values with that calculated from thermodynamic data suggests that steady-state Pu concentrations are controlled by kinetics. Possible pathways of secondary reactions are identified and a mechanism for reversible oxygenation of plutonium ions is described.

1. Introduction

Knowledge of plutonium oxidation states and speciation in solution is essential for describing process chemistry [1] and thermodynamic properties [2], as well as for evaluating behavior of Pu in the environment [3]. Solutions containing Pu(IV), Pu(V), or Pu(VI) are unstable due to disproportionation of plutonium in those oxidation states. Early studies show that Pu(IV) forms Pu(III), Pu(V), and Pu(VI) in acidic media [4–6]. Disproportionation of Pu(V) forms Pu(III) plus Pu(VI) in some cases [1,7] and Pu(IV) plus Pu(VI) in others [1,8,9] with reaction rates varying by more than 10^6 over the pH 0–15 range [10,11]. Recent studies show that disproportionation, not alpha-induced reduction by peroxide, is the primary pathway for Pu(VI) instability over a broad pH range [10,11]. Only Pu(V) is observed because Pu(VI) is reformed by immediate reduction of the highly reactive Pu(VII) disproportionation product by water.

Disproportionation of Pu(IV) is described in several studies with acidic perchlorate [4,5,12], chloride [4,12–14] and nitrate [6,15,16] solutions.

* Tel.: +1 254 399 0740; fax: +1 254 399 8876.
E-mail address: johnhaschke@msn.com

0022-3115/$ - see front matter © 2006 Elsevier B.V. All rights reserved.
doi:10.1016/j.jnucmat.2006.11.006

In 1 M H^+, the reaction is most accurately described by Eq. (1)

$$3Pu^{4+}\ (aq) + 2H_2O\ (l) \rightarrow 2Pu^{3+}\ (aq) + PuO_2^{2+}\ (aq) + 4H^+\ (aq) \qquad (1)$$

In an early work, Connick [13] concluded that Eq. (1) proceeds via a two-step sequence of bimolecular reactions because mechanistic steps involving three or more plutonium ions are of low probability. The proposed reaction path (Eqs. (2) and (3)) is adopted in subsequent studies [4–6,12–17].

$$2Pu^{4+}\ (aq) + 2H_2O\ (l) \rightarrow Pu^{3+}\ (aq) + PuO_2^{+}\ (aq) + 4H^+\ (aq) \qquad (slow) \qquad (2)$$

$$Pu^{4+}\ (aq) + PuO_2^{+}\ (aq) = Pu^{3+}\ (aq) + PuO_2^{2+}\ (aq) \qquad (fast) \qquad (3)$$

According to this mechanism, the rate-controlling step is followed by rapid reaction of Pu(V) product with Pu(IV) to establish an equilibrium state involving the four common Pu oxidation states [1,12,13]. Measurements show that the equilibrium constant for Eq. (1) is given by $K_1 = [Pu^{3+}]^2[PuO_2^{2+}][H^+]^4/[Pu^{4+}]^3$ or, more generally, by $[Pu(III)]^2[Pu(VI)][H^+]^4/[Pu(IV)]^3$ [5].

Formation of Pu(V) during Pu(IV) disproportionation is implied by failure of measured [Pu(III)], [Pu(IV)], and [Pu(VI)] to account for total Pu concentrations at pH 0.4–1.0 [6] and is shown by observation of Pu(V) over the 0.30–1.2 pH range [15,16]. According to the two-step mechanism, K_1 is defined by the product of K_2 for Eq. (2) and K_3 for Eq. (3) and is independent of [Pu(V)] because the $[PuO_2^+]$ terms in those expressions cancel [4,5]. However, as discussed previously [18], the net reaction of the two-step sequence fails to include Pu(V) as a product and fixes the equilibrium [Pu(III)]:[Pu(VI)] at 2:1. Reversibility of Eq. (1) near pH 0 is observed [7], but absence of detectable [Pu(V)] near zero time is inconsistent with the anticipated accumulation of that oxidation state during the rapid initial step.

The accepted value of K_1 (1 M $HClO_4$), the equilibrium constant for Eq. (1) in 1 M perchloric acid [2], is derived using concentrations present when $-d[Pu(IV)]/dt$ equals the rate at which Pu(IV) is reduced to Pu(III) by alpha-induced reaction [5]. The equilibrium constant obtained by this unconventional method is confirmed by the study of the Pu(III)–Pu(VI) reaction [7]. However, reliability of K_1 remains uncertain because stable concentrations are not observed for either the forward [5] or reverse [7] reactions. Available kinetic data do not provide an independent determination of K_1 because rate constants in one direction are based on measured equilibrium constants and rate constants for the opposing direction.

The present study was initiated in an effort to address inconsistencies cited above and to more accurately describe the solution chemistry of Pu(IV). Additional impetus for the effort arose from preliminary results showing that $-d[Pu(IV)]/dt$ is not proportional to $[Pu(IV)]^2$ as required for a bimolecular disproportionation reaction. In addition to examining kinetic and equilibrium properties of aqueous Pu(IV), this study provides new evidence that the redox chemistry of plutonium solutions is not determined by equilibrium thermodynamics, but by kinetically controlled reactions that depend on formation of hydroxide complexes [10,11,19]. The length of this report reflects the need to show both that prior interpretations are inadequate and that behavior is accurately described by an alternative approach.

2. Data sources and methods

Characterization of Pu(IV) disproportionation is based on evaluation of kinetic and equilibrium data from literature sources. Interpretation of behavior in non-complexing media is constrained by a limited amount of concentration–time ([Pu(IV)]–t) data for perchlorate solutions [5,7]. Therefore, assessment relies largely on more extensive graphical [6] and tabulated [15,16] results for nitrate solutions. Extraction of data from graphical sources was facilitated by digital scanning and enlargement. Estimated errors of ±5% in [Pu(IV)]–t in digitized results have negligible effects on calculated kinetic parameters and model predictions.

Reaction rates are derived from Δ[Pu]–Δt increments of spectroscopic [Pu]–t data for nitrate and perchlorate solutions. Dependence of R_{1F}, the disproportionation rate of Pu(IV) at constant pH, on [Pu(IV)] is described by $-d[Pu(IV)]/dt = k_{1F}[Pu(IV)]^n$. If reaction proceeds by a single pathway, the exponent n is an integer equal to the slope of the $\ln R_{1F}$–ln[Pu(IV)] curve. Likewise, the exponent for the reverse Pu(III)–Pu(VI) reaction is defined by $\ln R_{1R}$–ln[Pu(III) + Pu(VI)], where R_{1R} is the rate of Pu(IV) formation via the reverse of Eq. (1). Values of k_{1F} and k_{1R} were calculated using experimental data and derived $\ln R$–ln[Pu] relationships.

Table 1
Kinetic data for Eqs. (2) and (3) in $HClO_4$ solutions

Reaction	Rate expression	k ($l\,mol^{-1}\,s^{-1}$)	Reference
Eq. (2) forward	$k_{2F}[Pu(IV)]^2$	$2.5\times10^{-5}/[H^+]^3$	[20]
Eq. (2) reverse	$k_{2R}[Pu(III)][Pu(V)]$	$4.4\times10^{-2}[H^+]$	[20]
Eq. (3) forward	$k_{3F}[Pu(IV)][Pu(V)]$	35	[19]
Eq. (3) reverse	$k_{3R}[Pu(III)][Pu(VI)]$	2.7	[20]

The dependence of k_{1F} on $[H^+]$ is given by $k_{1F} = c_{1F}[H^+]^m$. Values of m and c_{1F} were determined from $\ln k_{1F}$–$\ln[H^+]$ data and used to derive k_{1F} (1 M H^+) and k_{1R} (1 M H^+), the rate constants in 1 M acid.

The time dependencies of [Pu(III)], [Pu(IV)], [Pu(V)], and [Pu(VI)] during disproportionation and formation of Pu(IV) were modeled by iterative numerical integration of rate expressions for evaluated kinetic pathways. Rate laws and data for modeling of the two-step mechanism are given in Table 1 [19,20]. Rate expressions and kinetic constants for alternative models are from evaluation of [Pu]–t and k–$[H^+]$ data. During modeling of the two-step process, reaction was incrementally advanced according to Eq. (2) at the R_{1F} calculated for the existing [Pu(IV)]. Conditions for the next increment were established by redistributing Pu(V) according to Eq. (3) and K_3. Similar methods were used in calculating concentration–time data for the reverse Pu(III)–Pu(VI) reaction. Rate constants for alternative single-step pathways were refined by systematic variation of k to maximize agreement of observed and predicted [Pu]–t data. The amount of Pu in all oxidation states was summed after each increment to verify conservation of mass.

Equilibrium concentrations of Pu oxidation states formed by disproportionation of Pu(IV) according to the two-step mechanism were calculated using data in Table 1. Percentages of Pu(III), Pu(IV), and Pu(VI) were derived by successive approximation to K_1 with the [Pu(III)]:[Pu(VI)] ratio fixed at 2:1 in accordance with Eq. (1). Results at each selected $[H^+]$ were combined with K_3 to derive corresponding [Pu(V)] percentages and final values were obtained by normalizing to 100% for conservation of mass.

3. Results and discussion

3.1. Reaction products and the equilibrium state in nitrate solutions

Characterization of steady-state products formed during Pu(IV) disproportionation is essential for determining the course of reaction. Compiled data for nitrate systems (Table 2) [6,15,16] show that the pH range for assessment is limited because measurable concentrations of reactant and products are observed only for $[H^+]$ in the 0.060–0.50 M range.

Table 2
Measured distributions of products formed during disproportionation of Pu(IV) in HNO_3 solutions

$[H^+]$ (M)	$[Pu]_0$[a] (mM)	Measured Pu concentrations (%)					K_3[b]	K_1 (1 M HNO_3)[b]	Data source
		Pu(III)	Pu(IV)	Pu(V)	Pu(VI)	Polymer			
0.50[c]	42.5	12.2 ± 1.5	83.3 ± 0.9	0.5 ± 0.2	3.6 ± 0.4	0.4 ± 0.1	1.0	0.6×10^{-4}	15
0.40	7.7	18	74	<1	9	–	–	1.8×10^{-4}	6
0.30	7.6	28	60	<1	14	–	–	4.1×10^{-4}	6
0.20	2.04	41	38	5	16	–	3.4	7.9×10^{-4}	6
0.10	2.25	55	19	12	16	–	3.5	7.1×10^{-4}	6
0.10[c]	17.0	46.5 ± 2.0	23.1 ± 2.6	8.0 ± 0.7	15.1 ± 1.1	8.4 ± 2.9	3.8	3.0×10^{-4}	15
0.10[d]	9.20	49.2	9.9	23.1	16.9	0.6	3.6	4.2×10^{-3}	16
0.075[c]	9.20	52.6 ± 1.1	14.8 ± 2.9	14.8 ± 2.5	16.7 ± 0.8	1.1 ± 0.0	4.0	4.6×10^{-4}	15
0.075[d]	9.33	39.1	4.1	20.5	12.7	23.7	5.9	8.9×10^{-3}	16
0.060[d]	9.34	9.8	−1.1[e]	8.3	4.6	77.9	>90[e]	–	16

[a] $[Pu]_0$ is the total Pu concentration present initially as Pu(IV).
[b] K_3 and K_1 (1 M HNO_3) are calculated from listed concentrations. These constants are given by $[Pu(III)][Pu(VI)]/[Pu(IV)][Pu(V)]$ and $[Pu(III)]^2[Pu(VI)][H^+]^4/[Pu(IV)]^3$, respectively.
[c] Uncertainties given on the lower line are standard errors in calculated averages of multiple measurements.
[d] Percentages are measured after an elapsed time of 15 h. Attainment of equilibrium was not reported [16], but [Pu]–t data indicate that a steady state was approached.
[e] A negative Pu(IV) percentage is given in the original report. K_3 is derived using percentages reported for an elapsed time of 3 h.

This window, which is inherently constrained at low pH by the strong $[H^+]$ dependence of the equilibrium point, is further restricted due to increasing loss of Pu(IV) as polymer with increasing pH where detailed evaluation is limited by polymer formation. Results from the study by Costanzo et al. [16] are of diminished value because spectral data were analyzed using a multi-component least-squares method that failed to conserve mass and gave negative concentrations in come cases.

Results in Table 2 assist in determining if the disproportionation chemistry of Pu(IV) is adequately described by Eqs. (2) and (3). Derived K_3 values are consistent with attainment of an equilibrium state involving Pu(III), Pu(IV), Pu(V), and Pu(VI) as specified by the two-step sequence. The difference between the average K_3 (4.0 ± 0.9) derived for 0.40–0.075 M HNO_3 range and that (13.0) for $HClO_4$ is small. A consistent increase in K_3 values with decreasing $[H^+]$ may result from variation in ionic strength. The average K_1 (1 M HNO_3) of $(4.9 \pm 2.5) \times 10^{-4}$ obtained from data of Artyukhin et al. [6] and Toth et al. [15] over the 0.40–0.075 M $[H^+]$ range differs substantially from an earlier value of 4×10^{-7} [18]. Disagreement of the average K_1 (1 M HNO_3) with values derived from data of Constanzo et al. [16] is consistent with their uncertain reliability.

Comparison (Table 3) of measured steady-state concentrations of the four coexisting Pu oxidation states in HNO_3 solutions with calculated equilibrium values based on data for $HClO_4$ solutions (Table 1) also shows that behavior is in general agreement with reaction by the two-step sequence. The observed extent of Pu(IV) disproportionation varies regularly with acidity, is somewhat less than predicted at high $[H^+]$, and exceeds expectation at low $[H^+]$. The steady-state percentages of Pu(III) and Pu(V) increase with increasing extent of reaction, but the Pu(VI) percentage remains surprisingly constant at about 16% over much of the $[H^+]$ range. Disproportionation of Pu(IV) via Eqs. (2) and (3) in nitrate solutions cannot be challenged on the basis of equilibrium results.

However, as discussed previously [18], the net equation must include Pu(V) as a product if reaction proceeds via the two-step sequence. Unlike an equation given in this earlier review, the following general relationship is independent of anion-specific equilibrium constants and applicable to all acid systems

$$(2+x)\mathrm{Pu}^{4+}\ (\mathrm{aq}) + 2\mathrm{H_2O}\ (\mathrm{l}) \rightarrow (1+x)\mathrm{Pu}^{3+}\ (\mathrm{aq}) + (1-x)\mathrm{PuO_2^+}\ (\mathrm{aq}) + x\mathrm{PuO_2^{2+}}\ (\mathrm{aq}) + 4\mathrm{H}^+\ (\mathrm{aq}) \quad (4)$$

Table 3
Comparison of observed steady-state properties with those calculated for disproportionation of Pu(IV) via Eqs. (2) and (3) in HNO_3 solution[a]

$[H^+]$	Steady-state Pu concentration (%)[b]								r_c[c]	N[d] (moles)	x[d]
	Pu(III)		Pu(IV)		Pu(V)		Pu(VI)				
	Obs	Cal	Obs	Cal	Obs	Cal	Obs	Cal			
1.00	–	18.6	–	71.9	–	0.2	–	9.3	1.01	10.676	0.986
0.50	12.2	32.7	83.3	50.1	0.5	0.8	3.6	16.4	1.02	6.012	0.967
0.40	18	37.5	74	42.4	<1	1.3	9	18.8	1.04	5.208	0.956
0.30	28	43.0	60	32.3	<1	2.2	14	21.5	1.05	4.431	0.938
0.20	41	49.1	38	22.0	5	4.2	16	24.6	1.09	3.846	0.893
0.10	55	52.8	19	9.4	12	11.4	16	26.4	1.22	3.312	0.749
	50.8		25.2		8.7		16.5				
	49.2		9.9		23.1		16.9				
0.075	53.2	52.2	15.0	6.4	15.0	15.3	16.9	26.1	1.29	3.205	0.673
	51.2		5.4		26.8		16.6				
0.060	44.3	49.3	0	4.3	37.6	21.8	20.8	24.6	1.44	3.135	0.544

[a] Observed Pu percentages correspond with values given in Table 2 and are normalized to account for Pu present as Pu(IV) polymer.
[b] Calculated percentages of Pu(III), Pu(IV), and Pu(VI) are based on the 2 Pu(III):1 Pu(VI) ratio of Eq. (1) and the value of K_1 determined by kinetic data for $HClO_4$ solutions in Table 1 ($K_1 = K_2K_3 = (k_{2F}/k_{2R})\ (k_{3F}/k_{3R} = 0.0086)$. Pu(V) percentages are derived from $[Pu(V)] = [Pu(III)][Pu(VI)]/K_3[Pu(IV)]$ and results are normalized to 100%.
[c] The charge-balance ratio is defined by $r_c = ([Pu(V)] + 2[Pu(VI)])/[Pu(III)]$.
[d] N and x are the requisite initial moles of Pu(IV) and the corresponding stoichiometric factor, respectively, necessary for reacting 3 moles of Pu(IV) and forming the calculated Pu(V) percentage according to Eq. (4).

Values of x vary with $[H^+]$ and approach 1 (negligible Pu(V)) in strong acid. Coefficients of Eq. (4) show that the moles of Pu(III) and Pu(VI) change by equal amounts (x) as the extent of Pu(V) formation varies. As $[H^+]$ decreases from 0.40 to 0.075 M, approximately 35% of the Pu is transformed to Pu(III) and [Pu(V)] increases from <1% to about 20%, but [Pu(VI)] increases by less than 10% over this range. Other implications of Eq. (4) are also disconcerting because K_4 is defined by non-integral concentration exponents that vary continuously with $[H^+]$ and are not readily correlated.

Reaction stoichiometry (Eq. (1)), equilibrium constants ($K_1 = K_2K_3$), mass balance, and charge balance must be simultaneously satisfied at equilibrium. Values of r_c, the ratio defined by [Pu(V)] + 2[Pu(VI)]/[Pu(III)], show that charge is not balanced in the two-step process if equilibrium concentrations are derived by fixing other parameters. Ratios based on calculated percentages (Table 3) exceed the required value of 1 and progressively increase with increasing Pu(V) percentage. Similar results (Table 3) are obtained if the calculated percentages of Pu(IV) lost and Pu(V) formed are used in deriving corresponding values of N and x for reaction according to Eq. (4). N is the initial moles of Pu(IV) necessary for disproportionating 3 moles of that reactant. Charge is balanced by x, but mass is not conserved because the moles of Pu product $(2 + x)$ do not equal 3. A prior derivation [18] of equilibrium percentages for 0.5 M HCl (26.4% Pu, 60.0% Pu(IV), 0.7% Pu(V), 12.9% Pu(VI)) shows that the Pu(III):Pu(VI) ratio is not 2:1 if Pu(V) is included and mass and charge are conserved. The two-step pathway is inherently flawed because all fundamental requirements are not simultaneously satisfied.

3.2. Disproportionation kinetics of Pu(IV) in nitrate solutions

As shown by $\ln R$–ln[Pu(IV)] analysis of experimental [Pu(IV)]–t data for nitrate solutions with different $[H^+]$ [6,16] (Fig. 1), dependence of the Pu(IV) disproportionation rate on [Pu(IV)] is third order. Data points (solid symbols) conform to lines with ideal slopes of 3 and are clearly inconsistent with a slope of 2 (line without data points) required for a bimolecular reaction. Linear least-squares refinements of results for solutions with 0.10, 0.20, and 0.30 M $[H^+]$ give respective n values of 2.9 ± 0.3, 3.2 ± 0.3, and 3.8 ± 0.7. A somewhat higher slope

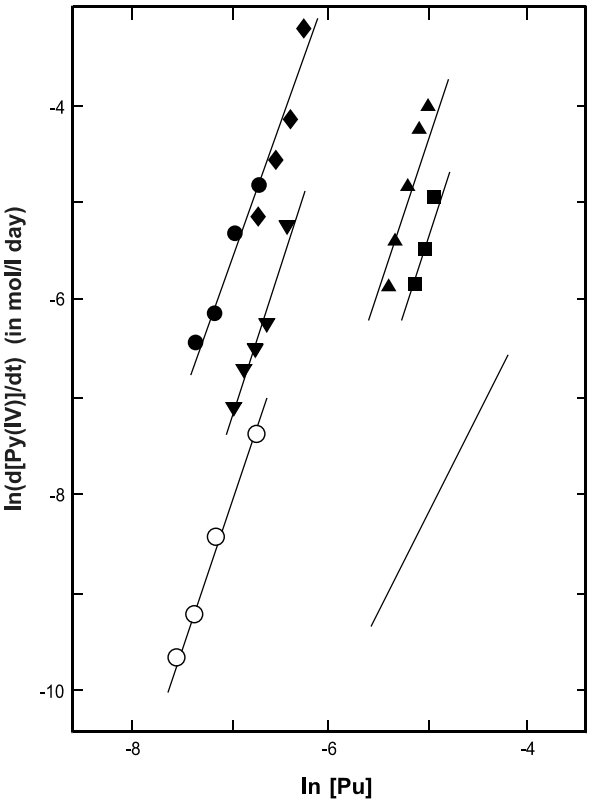

Fig. 1. Dependence of d([Pu(IV)])/dt on [Pu] during disproportionation of Pu(IV) (solid symbols) and formation of Pu(IV) via the Pu(III)–Pu(VI) reaction (open symbols) in acidic solutions. Solid circles [6] and diamonds [16], inverted solid triangles [6], upright solid triangles [6], and solid squares [6] describe data for 0.10, 0.20, 0.30 and 0.40 M HNO_3, respectively. Open circles describe data for 1.3 M $HClO_4$ [7]. Lines with data points have theoretical slopes of 3; the line without data points has a slope of 2.

is suggested by the limited data for 0.40 M $[H^+]$. Values of k_{1F} derived from the curves in Fig. 1 are given in Table 4.

Correlation of $\ln k_{1F}$ with $\ln[H^+]$ (Fig. 2) shows a complex acidity dependence of rate constants for Pu(IV) disproportionation. Interpretation is uncertain because data for nitrate solutions (open symbols) can be treated either as one set or as two sets. The least-squares slope of -4.4 ± 0.8 for a single set indicates that R_{1F} is proportional to $[H^+]^{-4}$ or $[H^+]^{-5}$, an acidity dependence equal to or greater than that of the overall reaction. The second option (Fig. 2) shows that the k_{1F} values are consistent with two lines of ideal slope -3 and a rate discontinuity near 0.25 M $[H^+]$. Preference is given to the later interpretation because $m = -3$ is reported in an earlier study with 0.2–1.0 M $HClO_4$ solutions [5] and because k_{1F} values (solid symbols) derived from

Table 4
Derived kinetic constants for disproportionation of Pu(IV) in nitrate solutions

$[H^+]$(M)	$\ln R_{1F}$–ln[Pu(IV)] analysis		[Pu]–t analysis
	k_{1F} ($l^2\,mol^{-2}\,d^{-1}$)	c_{1F} ($mol\,l^{-1}\,d^{-1}$)	k_{1F} ($l^2\,mol^{-2}\,d^{-1}$)
0.40	1.5×10^4	9.5×10^2	8.0×10^3
0.30	4.0×10^4	1.1×10^3	2.8×10^4
0.20	8.9×10^5	7.9×10^3	6.0×10^5
0.10[a]	4.9×10^6	4.9×10^3	3.5×10^6

[a] The k_{1F} from $\ln R_{1F}$–ln[Pu(IV)] analysis is based on the combined data set of solid circles [6] and solid diamonds [16]; that from [Pu]–t analysis is based only on data from Artyukhin et al. [6].

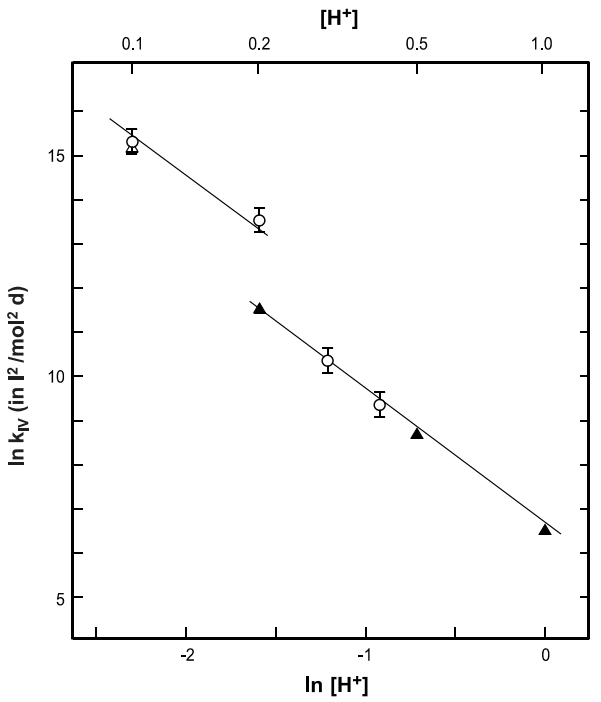

Fig. 2. Dependence of derived trimolecular rate constants for disproportionation of Pu(IV) on $[H^+]$. Open circles and triangle are for HNO_3 solutions. Solid triangles are for $HClO_4$ solutions.

results of that work (Section 3.4) agree with those for HNO_3 solutions.

Results show that the rate law for Pu(IV) disproportionation in acidic nitrate solutions is best described as follows:

$$R_{1F} = c_{1F}[\mathrm{Pu(IV)}]^3[H^+]^{-3} \quad (5)$$

Values of c_{1F} that are $(1.0\pm0.7)\times10^3\,mol\,l^{-1}\,d^{-1}$ for $[H^+]$ greater than 0.25 M and $(6.4\pm1.5)\times10^3\,mol\,l^{-1}\,d^{-1}$ for lower $[H^+]$ indicate the magnitude of the rate discontinuity in Fig. 2, but not its origin. The third-order dependence on [Pu(IV)] is inconsistent with a bimolecular rate controlling step (Eq. (2)) and implies that disproportionation proceeds via a trimolecular rate-determining step in accordance with Eq. (1).

3.3. Modeling of Pu(IV) disproportionation in nitrate solutions

3.3.1. Concentration–time results for reaction via Eqs. (2) and (3)

Calculated concentration–time curves for two-step disproportionation of Pu(IV) in 0.20 M HNO_3 are compared with experimental results [6] in Fig. 3. Data points for Pu(III), Pu(IV), and Pu(VI) show that concentrations change until a steady state is reached near 0.8 days. Steady-state concentrations of these oxidation states account for 95% of the Pu and imply that 5% is present as Pu(V). Although calculated curves are based on kinetic constants for $HClO_4$ solutions (Table 1),

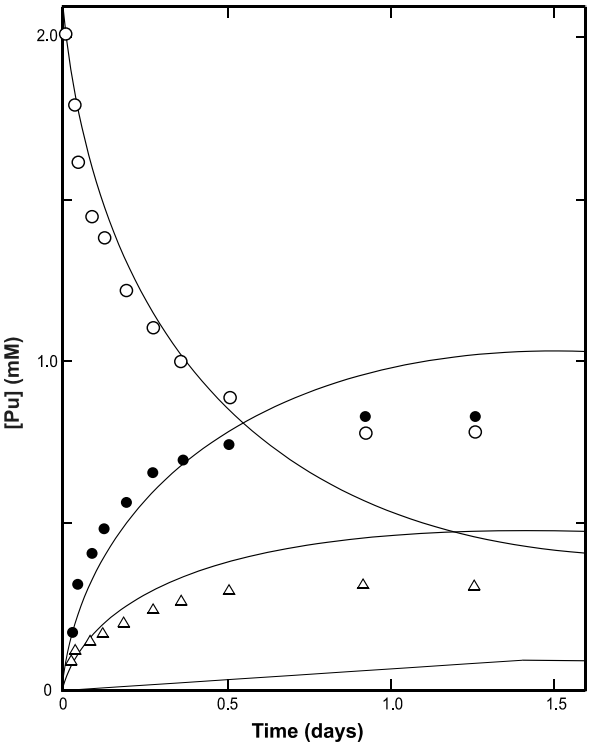

Fig. 3. Comparison of experimental data for disproportionation of Pu(IV) in 0.20 M HNO_3 [6] with [Pu]–t curves calculated for two-step bimolecular reaction via Eqs. (2) and (3). Values of [Pu(III)], [Pu(IV)], and [Pu(VI)] are indicated by solid circles, open circles, and open triangles, respectively.

agreement of k_{1F} values for nitrate and perchlorate (Fig. 2) indicate that disproportionation kinetics of Pu(IV) are anion insensitive.

Predicted curves for Pu(III) and Pu(IV) correspond well with data during the initial time period, but deviate with increasing time and then intersect near 0.4 day. Discrepancies increase at longer time with prediction accounting for only 75% of the measured steady-state Pu(IV) at 0.8 day. This difference and that for Pu(III) are reduced by using smaller k_{1F} values, but initial deviations are increased. That result is unavoidable because curve shape is fixed by the second-order rate law and does not match the time dependence of the data. The predicted curve for Pu(VI) intersects with data after 0.05 days and exceeds measured values at longer time.

As shown by the calculated curve without data points in Fig. 3, the [Pu(V)] is expected to increase over time until a steady state is established after 1.4 days. The derived percentages of Pu(III), Pu(IV), Pu(V), and Pu(VI) present when forward and reverse rates became equal (50.7%, 22.4%, 4.0% and 23.3%, respectively) differ slightly from calculated equilibrium values in Table 3. The Pu(V) percentage derived by kinetic modeling is in good agreement with the 5% deficit in the total [Pu], but the time dependence of [Pu(V)] is not consistent with prediction. For example, the calculated Pu(V) percentage of 1% at 0.5 day is substantially less than the experimental value of 4%. Although the two-step mechanism cannot be rejected on the basis of [Pu]–t results in Fig. 3, its failure to satisfy fundamental requirements is again evident because the total [Pu] after each iterative calculation exceeded the initial value and normalization of concentrations after each iteration was necessary to maintain mass balance.

3.3.2. Concentration–time results for reaction via Eq. (1)

Concentration–time curves for single-step disproportionation of Pu(IV) in 0.20 M HNO_3 are derived by integration of Eq. (5) and are compared with experimental results [6] in Fig. 4. Predicted curves for Pu(III) and Pu(IV) correspond closely with data until the steady state is reached at 0.8 day. Measured Pu(VI) concentrations are consistently less than expected and account for a constant fraction ($77 \pm 4\%$) of the predicted [Pu(VI)] during the initial 0.8 day period. Comparison of calculated and experimental data [6] for a 0.10 M H^+ solution gives

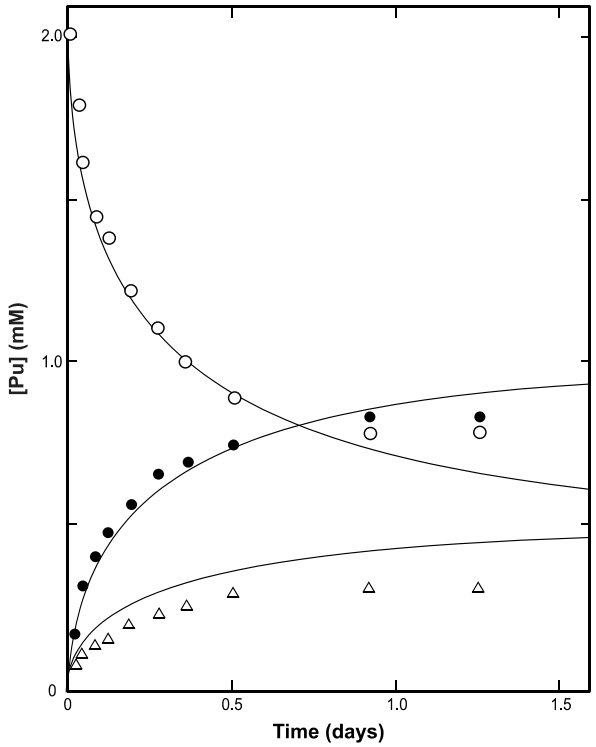

Fig. 4. Comparison of experimental data for disproportionation of Pu(IV) in 0.20 M HNO_3 [6] with [Pu]–t curves calculated for single-step trimolecular reaction via Eq. (1). Values of [Pu(III)], [Pu(IV)], and [Pu(VI)] are indicated by solid circles, open circles, and open triangles, respectively.

parallel results with the measured [Pu(VI)] equal to $71 \pm 3\%$ of the predicted value. Within a factor of two, k_{1F} values (Table 4) derived by fitting [Pu]–t data (Table 4) agree with those obtained from $\ln R_{1F}$–ln[Pu(IV)] analysis.

Results imply that disproportionation proceeds via Eq. (1) and that Pu(V) is formed solely from the Pu(VI) product via a secondary reaction. [Pu]–t curves in Fig. 4 demonstrate that the molar ratio of Pu(III) formed to Pu(IV) lost is 2:3, a result consistent with Eq. (1). Maintenance of charge balance requires that the molar ratio of Pu(VI) formed to Pu(IV) lost be 1:3, but observed ratios are about 0.75:3. Experimental values of r_c for 0.10 and 0.20 M [H^+] are 0.855 and 0.885, respectively, implying that Pu(VI) is reduced to Pu(V). This conclusion is supported by values of ([Pu(V)] + [Pu(VI)])/[Pu(III)], a ratio that equals 0.5 if the initial reaction proceeds according to Eq. (1) and reduction of Pu(VI) to Pu(V) is the only secondary reaction. Variable ratios with values greater than 0.5 are expected if Pu(V) is formed via Eq. (4).

Disproportionation of Pu(IV) in solutions with 0.5–1.0 M $[H^+]$ produce negligible amounts of Pu(V) and is accurately described by Eq. (1) [5]. Ratios for these solutions are 0.50. Steady-state concentrations for solutions with 0.40 [6], 0.30 [6], 0.20 [6], 0.10 [6], and 0.10 M [15] $[H^+]$ (Table 2) give ratios of 0.50, 0.50, 0.51, 0.51, and 0.50, respectively, demonstrating that observed amounts of Pu(V) accurately account for observed deficits in Pu(VI).

Disproportionation of Pu(VI) yields Pu(V) as the only product over a wide pH range [10,11]. Occurrence of that reaction provides a possible explanation for forming Pu(V) directly from Pu(VI), but kinetic analysis does not support that conclusion. Results (Fig. 4) show that Pu(V) formed at a rate greater than 3×10^{-5} mol l^{-1} d^{-1} and that the deficit in [Pu(VI)] did not increase detectably during the four day period after the steady state was reached [6]. Application of kinetic data [10] to the steady-state 0.20 M H^+ solution with 3×10^{-4} M [Pu(VI)] gives a disproportionation rate (2×10^{-6} mol l^{-1} d^{-1}) consistent with a time-insensitive [Pu(VI)] beyond 0.8 day, but unable to account for the relatively rapid formation of Pu(V) at shorter times. The rate of Pu(V) formation tracks the rate of Pu(IV) disproportionation, suggesting that products of the slow step are involved. Coincidence of the rate discontinuity (Fig. 2) with appearance of substantial Pu(V) near 0.2 M H^+ may be important or only fortuitous. Although the chemistry of Pu(V) formation is not fully defined, observations are consistent with disproportionation of Pu(IV) via a single-step trimolecular reaction that proceeds according to Eq. (1) and indirectly produces Pu(V).

3.4. Disproportionation kinetics of Pu(IV) in perchlorate solutions

Modified methods are necessary for evaluating kinetic behavior in perchlorate solutions because [Pu]–t data are not included in reports on Pu(IV) disproportionation [4,5]. Formation of Pu(V) is negligible in 0.5–1.0 M $HClO_4$ and reaction is described by Eq. (1) [5]. Therefore, the adopted approach uses the linear $\ln R_{1F}$–ln[Pu(IV)] relationship with $n = 3$ and with the assumption that the reaction rate near zero time is adequately defined by the binary rate law. A k_{1F} value of 630 l^2 mol^{-2} d^{-1} is obtained using the average rate (6.3×10^{-3} mol l^{-1} d^{-1}) calculated for the initial 5% of reaction in a 1.0 M $HClO_4$ solution with a $[Pu(IV)]_0$ of 11.0 mM.

An alternative approach that supports the third-order rate law and independently yields k_{1F} is based on modeling of [Pu]–t data generated using the binary rate law and Eq. (1) [5,19]. Values of [Pu(III)], [Pu(IV)], and [Pu(VI)] calculated as a function of time for 11.0 mM Pu(IV) in 1 M $HClO_4$ are shown by data points in Fig. 5. Curves derived by integration of Eq. (5) with a k_{1F} value of 690 l^2 mol^{-2} d^{-1} describe the time dependencies of all Pu ions with surprising accuracy beyond the calculated equilibrium point (18.7% Pu(III), 71.9% Pu(IV), and 9.4% Pu(VI) at 4.6 days) of the two-step model. In large measure, success of this method results from absence of sharp curvature in data for a limited-extent reaction. Evaluation of data for 0.50 and 0.20 M $HClO_4$ yield k_{1F} values of 6.2×10^3 and 1.0×10^5 l^2 mol^{-2} d^{-1}, respectively. As shown in Fig. 2, the third-order rate constants for perchloric acid solutions form a single data set with those for nitric acid solutions and confirm the third-order dependence of k_{1F} on $[H^+]$.

The rate law for Pu(IV) disproportionation in perchloric acid is described by Eq. (5). Values of c_{1F} derived for 1.0, 0.5, and 0.2 M acid (690, 775 and 800 mol l^{-1} d^{-1}, respectively) show a slight

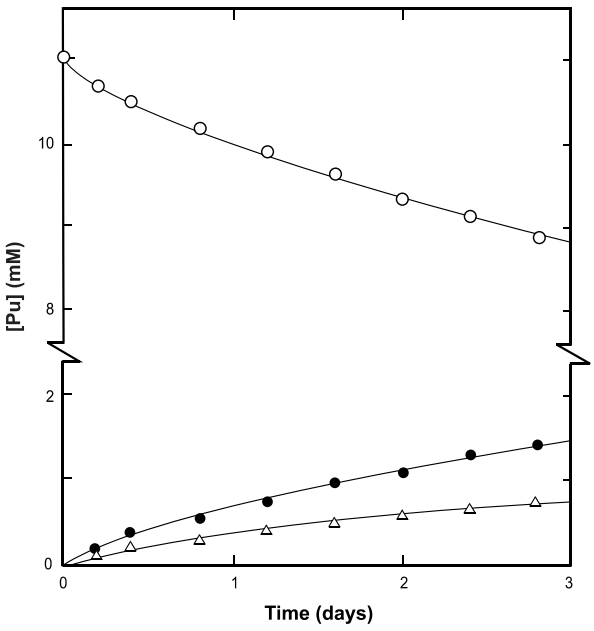

Fig. 5. Fitting Pu(IV) disproportionation data generated for the two-step bimolecular reaction sequence with curves calculated for single-step trimolecular reaction. Values of [Pu(III)], [Pu(IV)], and [Pu(VI)] are indicated by solid circles, open circles, and open triangles, respectively.

trend with $[H^+]$. Preference is given to an average c_{1F} of 660 mol l^{-1} d^{-1} obtained from results for 1.0 M $[H^+]$.

3.5. Chemistry and kinetics the Pu(III)–Pu(VI) reaction in perchlorate solution

A kinetic study of the reaction between Pu(III) and Pu(VI) by Capdevila et al. [7] is important in describing the chemistry of Pu(IV) disproportionation. Spectroscopic [Pu]–t data are reported for reactants and products during reaction in 1.3 M $HClO_4$ ($[Pu(III)]_0$, $[Pu(IV)]_0$, and $[Pu(IV)]_0$ values of 0.90, 0.23, and 0.58 mM, respectively) over a 30 day period in Fig. 6. Pu(V) was not initially present. Data show that 70% of the Pu(III) reacted with Pu(VI) in a 2:1 ratio to form Pu(IV) (reverse of Eq. (1)) during the initial 4.5 days. As the Pu(VI) concentration continued to decrease over the test period, values of [Pu(III)] and [Pu(IV)] remained essentially static for several days before beginning to increase and decrease, respectively. Failure to detect a measurable [Pu(V)] during reaction or at steady state cannot be attributed to inadequate spectroscopic methods. The capability for determining the Pu(V) concentration in the presence of Pu(III) is shown by results of a companion investigation of Pu(V) disproportionation [7] and by other studies [15,16]. Results conflict with earlier reports by Rabideau and Klein [19] and by Lavallee and Newton [17] that the Pu(III)–Pu(VI) reaction proceeds to equilibrium by reversal of the two-step reaction.

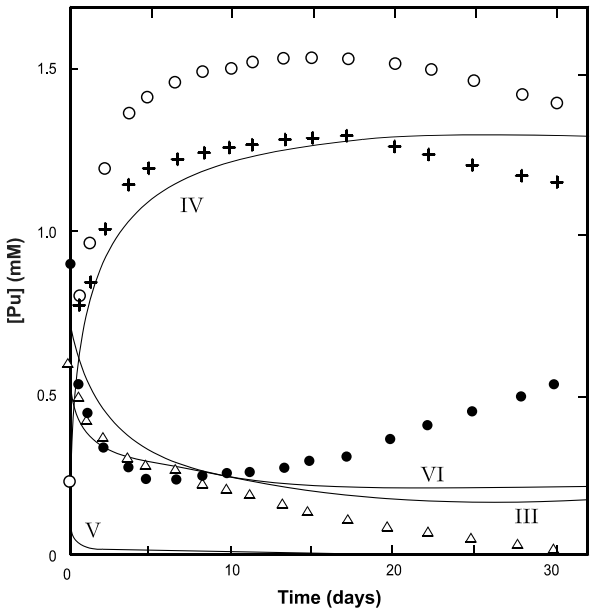

Fig. 6. Comparison of experimental data for formation of Pu(IV) by the Pu(III)–Pu(VI) reaction in 1.3 M $HClO_4$ [7] with [Pu]–t curves calculated for two-step bimolecular reaction via Eqs. (2) and (3). Reported values of [Pu(III)], [Pu(IV)], and [Pu(VI)] are indicated by solid circles, open circles, and open triangles, respectively. Recalculated values of [Pu(IV)] are indicated by plus symbols.

Correction of the [Pu]–t data of Capdevila et al. [7] is necessary because the total [Pu] progressively increased by 15% beyond the $[Pu]_0$ of 1.71 mM l^{-1} during the first 10 days and thereafter remained constant at an average of 1.97 ± 0.01 mM l^{-1}. Evaluation suggests that the increase results from a shift in analytical calibration for [Pu(IV)]. Calculation of [Pu(IV)]–t from measured decreases in [Pu(III)]–t and [Pu(VI)]–t gives a constant total [Pu] throughout the test period.

The general rate equation for formation of Pu(IV) in a single step via the reverse of Eq. (1) is given by $+d[Pu(IV)]/dt = R_{1R} = k_{1R}[Pu(III)]^{v}[Pu(IV)]^{\omega}$. The slope obtained by $\ln R_{1R}$–$\ln([Pu(III)] + [Pu(VI)])$ analysis of data [7] in Fig. 1 shows that $(v + \omega) = 3$. Testing of possible v and ω combinations using incremental rates and concentrations from the initial 4 h of measurement [7] give time-dependent k values for all rate-law permutations except that with $v = 2$ and $\omega = 1$. The k_{1R} value of $(3.5 \pm 0.6) \times 10^6$ l^2 mol^{-2} d^{-1} is obtained using these exponents and [Pu(IV)]–t data. Calculations based on measured [Pu(III)]–t data, on [Pu(VI)]–t data, and on corrected [Pu(IV)]–t data give respective k_{1R} values of $(1.4 \pm 0.2) \times 10^6$, $(1.5 \pm 0.4) \times 10^6$, and $(2.3 \pm 0.2) \times 10^6$ l^2 mol^{-2} d^{-1} and an average of $(1.7 \pm 1.1) \times 10^6$ l^2 mol^{-2} d^{-1} for the third-order rate constant in 1.3 M $HClO_4$.

In the absence of data for other acid concentrations, a first-order dependence of k_{1R} on $[H^+]$ is inferred by $m = -3$ and the fourth-order $[H^+]$ dependence of K_1 [5]. Therefore, the rate law for formation of Pu(IV) by the Pu(III)–Pu(VI) reaction in perchloric acid solutions is described as follows:

$$R_{1R} = c_{1R}[Pu(III)]^2[Pu(IV)][H^+] \quad (6)$$

The derived value of c_{1R} is $(1.3 \pm 0.5) \times 10^6$ l^3 mol^{-3} d^{-1}. Eq. (6) and the rate law for Pu(IV) disproportionation (Eq. (5)) support earlier conclusions that Eq. (1) is reversible [5], but are inconsistent with a bimolecular rate-controlling step.

3.6. Modeling of the Pu(III)–Pu(VI) reaction in perchlorate solutions

3.6.1. Concentration–time results for Pu(IV) formation via Eqs. (3) and (2)

Experimental results for the Pu(III)–Pu(VI) reaction in 1.3 M $HClO_4$ are compared with calculated [Pu]–t curves for formation of Pu(IV) by the two-step reaction sequence in Fig. 6. Reported [Pu(IV)]–t data [7] are shown by open circles and corrected values are indicated by plus symbols. Meaningful comparison is limited to the first 4.5 day period in which secondary reactions are insignificant. The first step of the formation reaction (reverse of Eq. (3)) is rapid and the calculated equilibrium point ($K_3 = 0.077$) is attained after 2.9 min. The calculated concentrations of Pu(III) and Pu(VI) decrease by 0.094 mM and those of Pu(IV) and Pu(V) increase by that amount. Curves in Fig. 6 are derived by incremental advancement of reaction according to the reverse of Eq. (2), followed by redistribution of products to again satisfy K_3. The theoretical equilibrium point ($K_2 = 0.0086$) is reached after 20 days with [Pu(III)], [Pu(IV)], [Pu(V)], and [Pu(VI)] values of 0.18, 1.31, 0.002, and 0.22 mM, respectively.

As in the similar evaluation of the two-step disproportionation reaction (Fig. 3), calculated [Pu]–t curves for the Pu(III)–Pu(VI) reaction in Fig. 6 do not coincide closely with the data, especially near zero time where formation of substantial Pu(V) is expected. A possible explanation for observed discrepancies is that the initial concentrations were measured after the equilibrium state for Eq. (3) had been reached. That possibility can be rejected because the zero time [Pu(V)] (0.17 mM) required for satisfying K_3 is not observed. That [Pu(V)] and the anticipated equilibrium value (0.094 mM) indicated in Fig. 6, are well within the analytical capability [7]. Absence of Pu(V) demonstrates that the Pu(III)–Pu(VI) reaction does not proceed by the two-step pathway. Inadequacy of the concept is further shown by failure of mass conservation during modeling calculations.

The conflict between results of Capdevila et al. (Fig. 6) and findings of earlier work [17,19] cannot be resolved. Rabideau and Kline [19] measured kinetics of Pu(IV) formation in 0.1–1.0 M $HClO_4$ with $[Pu(III)]_0$ and $[Pu(VI)]_0$ in a 10:1 ratio and report equal reaction rates in accordance with Eq. (3). This result and formation of Pu(V) are confirmed by Lavallee and Newton [17]. Use of unequal reactant concentrations may be a factor because a 1:1 Pu(III):Pu(VI) reaction ratio would result if the measured [Pu(III)] were too high by 10%. Pu(V) may form by secondary reaction under appropriate conditions, but evaluation is precluded by unavailability of data.

3.6.2. Concentration–time results for Pu(IV) formation via Eq. (1)

Concentration–time curves for single-step formation of Pu(IV) by the Pu(III)–Pu(VI) reaction in 1.3 M $HClO_4$ are derived by integration of Eq. (6). Comparison of the results with experimental data in Fig. 7 [7] shows close agreement during the first 4.5 days. The need for correction of [Pu(IV)]–t data is shown by correspondence of those values with the predicted curve. Results confirm that kinetic behavior is consistent with formation of Pu(IV) via a reversible trimolecular process according to Eq. (1).

Deviation of the predicted [Pu]–t curves from the experimental data (Fig. 6) identifies 4.5 days as the point beyond which kinetic behavior is determined by secondary reaction(s). At that time, the [Pu(III)] begins to increase, [Pu(IV)] begins to decrease, and [Pu(VI)] continues to decrease at a rate faster than

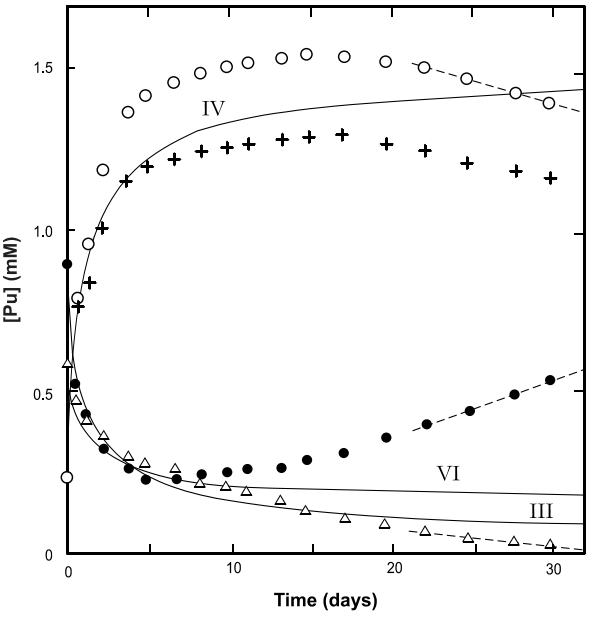

Fig. 7. Comparison of experimental data for formation of Pu(IV) by the Pu(III)–Pu(VI) reaction in 1.3 M $HClO_4$ [7] with [Pu]–t curves calculated for single-step trimolecular reaction via Eq. (1). Reported values of [Pu(III)], [Pu(IV)], and [Pu(VI)] are indicated by solid circles, open circles, and open triangles, respectively. Recalculated values of [Pu(IV)] are indicated by plus symbols.

predicted by Eq. (6). As defined by the slopes of the lines through data points in Fig. 7, average rates of Pu(VI) and Pu(IV) consumption and Pu(III) formation during the day 25 to day 30 period are 4.6×10^{-6}, 13.7×10^{-6}, and 18.3×10^{-6} mol l^{-1} d^{-1}, respectively. Rate ratios show that reaction of 1 Pu(VI) and 3 Pu(IV) produces 4 Pu(III). The net reaction does not simply redistribute electrons because charges do not balance. The nature of the reaction and the origin of near-static concentrations identified as the equilibrium state [7] is suggested by comparing the Pu(VI) reaction rate at 4.5 day (8.7×10^{-6} mol l^{-1} d^{-1}) with that (8.8×10^{-6} mol l^{-1} d^{-1}) calculated for reduction of Pu(VI) to Pu(V) by disproportion-driven reaction of 0.28 mM Pu(VI) in 1.3 M acid [10]. The Pu(VII) product formed by Pu(VI) disproportionation is instantaneously reduced back to Pu(VI) by reaction with H_2O and Pu(V) remains as the only observed product. This process is more rapid than the Pu(III)–Pu(VI) reaction beyond 4.5 days and determines long-term chemistry.

Two pathways for the secondary redox process (Table 5) are consistent with apparent involvement of disproportionation-driven Pu(VI) reduction. Values of $-d[Pu(VI)]/dt$ derived from the [Pu(VI)]–t data for day 5 to day 30 (Fig. 7) agree with rates calculated for disproportionation of Pu(IV). Secondary reaction is apparently triggered when the Pu(VI) disproportionation rate exceeds the rate of Pu(VI) loss via the Pu(III)–Pu(VI) reaction. As shown by adding Eqs. (5A) and (5B) or Eqs. (5A) and (5E), repeated addition of electrons to the Pu system by disproportionation-driven Pu(VI) reduction ultimately produces Pu(III) and shifts Eq. (1) in the reverse direction. These reactions also form Pu(VI) that is recycled into the reduction process (Eq. (5A)). Both pathways account for the observed stoichiometry (Eq. (5D)) and may contribute to the rate.

Another repeated step in the second reaction sequence (Table 5) is the redox reaction of Pu(IV) and Pu(V) according to Eq. (3). Occurrence of this reaction is not precluded by results [7] showing that the reaction is not reversible in 1.3 M $HClO_4$.

3.7. Reaction mechanisms

Consideration of constraints imposed by observed dependencies of the rates on concentrations of Pu cations and H^+ provides valuable insight into the complex redox chemistry of Pu. Reaction is predicated on association of Pu cations in a configuration that facilitates electron transfer, but formation of that reactive intermediate is inherently constrained by cationic repulsion. Hydrolysis is a pH-dependent process that reduces cationic charge on Pu cations and increases the likelihood of polymerization. As demonstrated by formation of plutonium polymer in 0.5 M H^+ and less acidic solutions (Table 2), monomeric plutonium hydroxides form polynuclear hydroxo complexes that bind Pu atoms in potentially reactive configurations. The mechanism proposed for Eq. (1) in an earlier study [5] does

Table 5
Equation sequences describing the secondary redox reaction observed in 1.3 M $HClO_4$[a]

		Ref.
Sequence involving disproportionation reactions of Pu(IV) and Pu(V)		
(5A)	$6(Pu(VI)\ (aq) + 1/2H_2O\ (l) \rightarrow Pu(V)\ (aq) + H^+\ (aq) + 1/4O_2\ (g))$	[10,11]
(5B)	$2(3Pu(V)\ (aq) \rightarrow Pu(III)\ (aq) + 2Pu(VI)\ (aq))$	[7]
(5C)	$3Pu(IV)\ (aq) \rightarrow 2Pu(III)\ (aq) + Pu(VI)\ (aq)$	[1,5]
(5D)	$3Pu(IV)\ (aq) + Pu(VI)\ (aq) + 3H_2O\ (l) \rightarrow 4Pu(III)\ (aq) + 6H^+\ (aq) + 3/2O_2\ (g)$	
Sequence involving reaction of Pu(IV) and Pu(V) and disproportionation of Pu(V)		
(5A)	$6(Pu(VI)\ (aq) + 1/2H_2O\ (l) \rightarrow Pu(V)\ (aq) + H^+\ (aq) + 1/4O_2\ (g))$	[10,11]
(5E)	$4(Pu(IV)\ (aq) + Pu(V)\ (aq) \rightarrow Pu(III)\ (aq) + Pu(VI)\ (aq))$	[5]
(5F)	$2Pu(IV)\ (aq) \rightarrow Pu(IV)\ (aq) + Pu(VI)\ (aq)$	[8,13]
(5D)	$3Pu(IV)\ (aq) + Pu(VI)\ (aq) + 3H_2O\ (l) \rightarrow 4Pu(III)\ (aq) + 6H^+\ (aq) + 3/2O_2\ (g)$	

[a] Equations are simplified by not including speciation of aqueous Pu oxidation states. In 1.3 M H^+, the primary aqueous species of Pu(III), Pu(IV), Pu(V), and Pu(VI) are Pu^{3+}, Pu^{4+}, PuO_2^+, and PuO_2^{2+}, respectively.

not account for the observed proportionality of R_{1F} to $[H^+]^{-3}$ [4] and involves formation of bimolecular intermediates with +5 charge.

Mechanistic pathways for forward and reverse reaction via Eq. (1) are derived using experimental dependencies of R_{1F} and R_{1R} on plutonium ion concentrations and $[H^+]$. The rate controlling steps in both directions are trimolecular and pH dependent. The proportionality of R_{1F} to $[H^+]^{-3}$ (Eq. (5)) implies that forward reaction proceeds by hydrolysis of aqueous Pu(IV) cations. Conversely, the direct dependence of R_{1R} on $[H^+]$ (Eq. (6)) implies that protonation of Pu ions is the dominant process in the Pu(III)–Pu(VI) reaction.

Mechanistic steps (Table 6) consistent with chemistry and experimental rate laws are formulated with $(PuOH)_3^{9+}$ as the reactive intermediate in both directions of Eq. (1) to demonstrate that kinetic constraints are satisfied by hydrolysis-driven formation of trimeric hydroxo complexes. Thermodynamic data [2] show that the equilibrium mole fraction of Pu(IV) existing as $PuOH^{3+}$ (aq) increases from 0.15 in 1 M H^+ to a maximum of 0.39 in 0.14 M H^+, and decreases slightly to 0.38 in 0.1 H^+. In the forward direction, a $(PuOH)_3^{9+}$ (aq) complex results from association of three $PuOH^{3+}$ (aq) ions with hydroxo bridging groups. In the reverse mechanism, hydroxo bridging groups are formed by protonation of PuO_2^{2+} (aq) (Eq. (6D)) and by hydrolysis of Pu^{3+} (aq) (Eq. (6E)).

Mechanisms in Table 6 show that observed dependencies of R_{1F} and R_{1R} on plutonium ion concentrations and $[H^+]$ are described by association of monomeric hydroxo complexes as trimeric reactive intermediates. However, formation of an intermediate with a +9 charge is energetically less favorable than association of less-highly-charged monomers. In the pH range of interest, four cations (Pu^{4+}, $PuOH^{3+}$, $Pu(OH)_2^{2+}$, and $Pu(OH)_3^+$) coexist in equilibrium [2] and their stepwise hydrolysis reactions occur simultaneously as described by the following general equation:

$$Pu(OH)_y^{(4-y)+}\ (aq) + H_2O\ (l) \rightarrow Pu(OH)_{y+1}^{(4-y-1)+}\ (aq) + H^+\ (aq) \quad (7)$$

Allowed values of y are integers in the 0–3 range with the distribution of hydrolysis products established by rapid equilibration at constant $[H^+]$. Eq. (6A) corresponds to the reaction for $y = 0$. The $Pu(OH)_3^+$ (aq) ion formed at $y = 2$ accounts for 4% of the Pu(IV) in 1 M H^+ and is predominant (41%) in 0.1 M H^+ [2]. Association of $Pu(OH)_3^+$ (aq) to form $(Pu(OH)_3)_3^{3+}$ (aq) is consistent with kinetic constraints and is energetically more favorable than Eq. (6B). Involvement of more than one cationic Pu(IV) hydroxo complex is possible with charges on the trimeric intermediates below 3+.

Development of a mechanism that accounts for a trimolecular intermediate in the Pu(III)–Pu(VI) reaction inherently involves a highly charged cationic intermediate because Pu^{3+} (aq) and PuO_2^{2+} (aq) are the predominant species in acidic solution [2]. Protonation of PuO_2^{2+} (aq) in accordance with proportionality of R_{1R} to $[H^+]$ increases the repulsive charge, but forms OH groups that are likely act as bridging groups in bonding of intrimeric intermediates. Protonation of dioxoplutonium ions

Table 6
Reaction mechanisms consistent with kinetic dependencies observed during disproportionation and reformation of Pu(IV) via Eq. (1)

Forward reaction

(6A) $3Pu^{4+}\ (aq) + 3H_2O\ (l) \rightarrow 3PuOH^{3+}\ (aq) + 3H^+\ (aq)$

(6B) $3PuOH^{3+}\ (aq) \rightarrow (PuOH)_3^{9+}\ (aq)$

(6C) $(PuOH)_3^{9+}\ (aq) \rightarrow 2Pu^{3+}\ (aq) + PuO_2^{2+}\ (aq) + H^+\ (aq) + H_2O\ (l)$

Reverse reaction

(6D) $PuO_2^{2+}\ (aq) + 2H^+\ (aq) \rightarrow Pu(OH)_2^{4+}\ (aq)$

(6E) $Pu^{3+}\ (aq) + H_2O\ (l) \rightarrow PuOH^{2+}\ (aq) + H^+\ (aq)$

(6F) $Pu^{3+}\ (aq) + PuOH^{2+}\ (aq) + Pu(OH)_2^{4+}\ (aq) \rightarrow (PuOH)_3^{9+}\ (aq)$

(6G) $(PuOH)_3^{9+}\ (aq) + 3H^+\ (aq) \rightarrow 3Pu^{4+}\ (aq) + 3H_2O\ (l)$

is not a new concept because the proportionalities of Pu(V) and Pu(VI) disproportionation rates to $[H^+]$ below pH 3 are attributed to protonation of PuO_2^+ (aq) and PuO_2^{2+} (aq) and involvement of $PuO(OH)^{2+}$ (aq) and $PuO(OH)^{3+}$ (aq) in forming bimolecular hydroxo complexes during rate-determining steps [11,8]. Low concentrations of $PuOH^{3+}$ (aq) and $Pu(OH)_2^{4+}$ (aq) in 1 M H^+ are consistent with limited formation of the reactive intermediate and with an R_{1R} that is almost 10^5 less than R_{1F}. Although protonated dioxoplutonium ions have not been characterized, a parallel reaction of H^+ with surface oxygen forms Pu–OH during dissociative chemisorption of water on PuO_2 (s) [21]. Concurrent binding of OH^- to surface Pu is analogous to the hydrolysis reactions of dioxoplutonium ions [2]. Amphoteric behavior of both PuO_2^+ (aq) and PuO_2^{2+} (aq) is implied by kinetic results and existence of protonated species in strong acid merits investigation.

In addition to describing observed kinetic behavior, the proposed mechanisms inherently account for the often-noted [1] slow formation of dioxoplutonium ions from Pu^{4+}, as well as for reversal of that process. As implied by Eq. (6C), disproportionation of Pu(IV) proceeds by electron transfer in linear or cyclic hydroxo trimer to form a species with a Pu(III)–OH–Pu(VI)–OH–Pu(III)–OH molecular skeleton and a net charge determined by y. In all cases, this intermediate dissociates to monomers and ultimately to Pu^{3+}(aq), PuO_2^{2+} (aq), H^+ (aq) and H_2O (l). This process is slow because the steady-state concentration of hydroxo trimer is low, but the reverse process that transforms PuO_2^{2+} (aq) back to Pu^{4+} (aq) is expected to be even slower.

The trimolecular mechanisms are idealized because the experimental exponents of Pu concentration are not constant. Values of n for forward reaction progressively increase from 3 to near 4 with increasing [Pu(IV)] (Fig. 1), while the dependence of R_{1F} on $[H^+]$ remains fixed with $m = -3$ (Fig. 2). The increase in n is consistent with increasing participation of another reactive species formed by association of the linear hydroxo trimer with Pu^{4+} via a singly-bonded OH. Effects of [Pu(IV)] on R_{1R} are not determined, but maintenance of a constant K_1 requires a corresponding increase in $v + \omega$ due to involvement of the higher complex.

The rate of Eq. (1) may be determined by formation of several polynuclear hydroxo intermediates corresponding to different values of y. The rather abrupt sixfold increase in R_{1F} near 0.2 M H^+ (Fig. 2) may result from an increase in the mole fraction of reactive hydroxo monomers as described by Eq. (6).

3.8. Equilibrium and thermodynamic properties

Reexamination of thermodynamic properties for Eq. (1) is merited because the accepted value of K_1 is defined by concentrations that existed when $-d[Pu(IV)]/dt$ was equal to the rate at which Pu(IV) is reduced to Pu(III) by alpha-particle radiolysis [5]. Although K_1 is confirmed by a subsequent study of the Pu(III)–Pu(VI) reaction [7], the basis for defining equilibrium is incorrect. Equilibrium is established when the rate of the forward reaction is equal to the rate of the reverse reaction, not when it is matched by the rate of a competing process. As described in Section 3.6.2, the near-static condition identified as the equilibrium point during the Pu(III)–Pu(VI) reaction [7] is reached when the rate of Pu(IV) loss via that process is matched by the disproportionation-driven rate of Pu(VI) reduction. Evaluation of kinetic information used for defining K_1 from data for disproportionation of Pu(IV) [5] shows that the reaction rate (1.4×10^{-4} mol l^{-1} d^{-1}) attributed to alpha reduction of Pu(IV) agrees with that (1.0×10^{-4} mol l^{-1} d^{-1}) calculated for Pu(VI) reduction [10] at the theoretical equilibrium [Pu(VI)] (1.1 mM) and pH 0. Fortuitously, the K_1 (1 M $HClO_4$) of 0.0089 based on alpha reduction [5] and that of 0.0081 defined by near-static concentrations during reverse reaction [7] are both fixed by the rates of Pu(VI) reduction at the test conditions.

Since attainment of the steady state for Eq. (1) is precluded by onset of secondary reaction in 1 M $HClO_4$, equilibrium is best defined by the point at which forward and reverse rates are equal. As given by c_{1F}/c_{1R} ($660/1.3 \times 10^6$), K_1 (1 M $HClO_4$) is $(5.1 \pm 2.2) \times 10^{-4}$. This result agrees with the K_1 (1 M HNO_3) of $(4.9 \pm 2.5) \times 10^{-4}$ obtained from steady-state concentrations measured in the 0.40–0.075 M $[H^+]$ range where the disproportionation-driven reduction rate of Pu(VI) is small. Theoretical equilibrium percentages of Pu(III), Pu(IV), and Pu(VI) in 1 M $HClO_4$ are 8.8%, 86.8%, and 4.4%, respectively. The derived ΔG (1 M $HClO_4$) of 18.8 ± 2.5 kJ mol^{-1} lies well beyond the uncertainty limits of the accepted value (11.68 ± 0.54 kJ mol^{-1}) [2].

Observations suggest that the steady states observed for solutions in the pH window are

determined by kinetics, not thermodynamics. The value of K_1 (1 M $HClO_4$) calculated from reference data with correction for ionic strength [2] is 0.063. The sevenfold difference between this result and the accepted K_1 (0.0089) might be attributed to inadequate ionic-strength correction, but that conclusion is meaningless in light of preceding discussion. The large discrepancy between the calculated K_1 and that derived in this study is consistent with control of the steady state by a kinetic process. Absence of thermodynamic control is also supported by agreement of K_1 (1 M HNO_3) and K_1 (1 M $HClO_4$) because stability of $PuNO_3^{3+}$ (aq) [2] should significantly shift the equilibrium point relative to that in a non-complexing perchlorate solution.

4. Conclusions

Kinetic data for disproportionation of Pu(IV) in acidic nitrate and perchlorate solutions via Eq. (1) are consistent with a single-step trimolecular reaction, not with the accepted two-step bimolecular reaction sequence. Pu(V) is neither a direct product of disproportionation nor a transient species in the reverse reaction of Pu(III) and Pu(VI), but forms by reduction of Pu(VI) product in a secondary process. The equilibrium state in which Pu(IV) and Pu(V) coexist with Pu(III) and Pu(VI) is not observed at conditions evaluated in this study. Instead, long-term redox products in strong acid are determined by pH-dependent secondary reactions in which electrons produced by disproportionation-driven reduction of Pu(VI) shift the average oxidation state toward III. The rate at which electrons are added to the Pu system by Pu(VI) reduction increases with decreasing pH and prevents attainment of the equilibrium state of Eq. (1) in acidic solutions. The rate of Pu(III) formation is ultimately determined by the rate of Pu(VI) reduction and accounts for the observation that rates attributed to alpha reduction of Pu(IV) and to alpha reduction of Pu(VI) are equal [20]. Stability of Pu(III) decreases with increasing pH [2], and as shown in Table 2, formation of Pu(IV) polymer becomes an increasingly important secondary reaction with decreasing acidity. Therefore, stable concentrations of the Pu ions that define K_1 are encountered only within a narrow window bounded by 0.40 and 0.075 M $[H^+]$.

Contrary to the view that reaction mechanisms are hypothetical and of uncertain value, results of this study provide clear evidence that reactive intermediates in the disproportionation and reformation reactions of Pu(IV) are polynuclear hydroxo complexes formed by association of monomeric products from hydrolysis and protonation reactions. Results for the Pu(III)–Pu(VI) reaction suggests that ions formed by protonation of PuO_2^{2+} are important chemical species in strong acid. Polynuclear hydroxo intermediates facilitate electron transfer by holding Pu atoms in close proximity; mechanistic pathways involving those intermediates inherently account for the chemistry and slow kinetics of reactions in which plutonium–oxygen bonds are formed and ruptured [1]. Failure of thermodynamic properties to describe steady-state behavior parallels earlier observations [10] indicating that redox chemistry of plutonium is controlled by kinetic factors.

Disproportionation of Pu(IV) forms Pu(VI), a kinetically unstable product that alters the long-term redox chemistry of Pu solutions. Additional investigation of the chemistry and kinetics of redox reactions over a wide pH range is necessary to account for non-equilibrium properties of steady-state solutions formed by PuO_2(c) and amorphous Pu(IV) hydrous oxide [22], and to assess the impact of disproportionation and other redox reactions on groundwater migration of Pu [3].

References

[1] J.M. Cleveland, The Chemistry of Plutonium, American Nuclear Society, La Grange Park, IL, 1979, p. 11.
[2] R.J. Lemire, J. Fuger, H. Nitsche, P. Potter, M.H. Rand, J. Rydberg, K. Spahiu, J.C. Sullivan, W.J. Ullman, P. Vitorge, H. Wanner, Chemical Thermodynamics of Neptunium and Plutonium, Elsevier, Amsterdam, 2001.
[3] R.J. Silva, H. Nitsche, Radiochim. Acta 70–71 (1995) 377.
[4] R.E. Connick, W.H. McVey, J. Am. Chem. Soc. 75 (1953) 474.
[5] S.W. Rabideau, J. Am. Chem. Soc. 75 (1953) 798.
[6] P.I. Artyukhin, V.I. Medvedovskvii, A.D. Gel'man, Russ. J. Inorg. Chem. 4 (1959) 596.
[7] H. Capdevila, P. Vitorge, E. Giffaut, Radiochim. Acta 58&59 (1992) 45.
[8] S.W. Rabideau, J. Am. Chem. Soc. 79 (1957) 6350.
[9] T.W. Newton, D.E. Hobart, D.P. Palmer, Radiochim. Acta 39 (1986) 139.
[10] J.M. Haschke, J. Nucl. Mater. 340 (2005) 299.
[11] J.M. Haschke, J. Nucl. Mater. 334 (2004) 225.
[12] S.W. Rabideau, L.B. Asprey, T.K. Keenen, T.W. Newton, in: Proceedings of the Second International Conference of Peaceful Uses of Atomic Energy, vol. 28, United Nations, Geneva, 1958, p. 261.
[13] R.E. Connick, J. Am. Chem. Soc. 71 (1949) 1528.
[14] S.W. Rabideau, H.D. Cowan, J. Am. Chem. Soc. 77 (1955) 6145.

[15] L.M. Toth, J.T. Bell, H.A. Friedman, Radiochim. Acta 49 (1990) 193.
[16] D.A. Costanzo, R.E. Biggers, J.T. Bell, J. Inorg. Nucl. Chem. 35 (1973) 609.
[17] C. Lavallee, T.W. Newton, Inorg. Chem. 11 (1972) 2616.
[18] J.J. Katz, G.T. Seaborg, L.R. Morss, second ed.The Chemistry of the Actinide Elements, vol. 1, Chapman&Hall, London, 1968, p. 820.
[19] S.W. Rabideau, R.J. Kline, J. Phys. Chem. 62 (1958) 617.
[20] T.W. Newton, Redox Reactions of Plutonium Ions in Aqueous Solutions, in: D.C. Hoffman (Ed.), Advances in Plutonium Chemistry 1967–2000, American Nuclear Society, La Grange Park, IL, 2002, p. 24.
[21] J.M. Haschke, J. Nucl. Mater. 344 (2005) 8.
[22] J.M. Haschke, R.L. Bassett, Radiochim. Acta 90 (2002) 505.